NMR determination of an incommensurate helical antiferromagnetic structure in EuCo_{2}As_{2}

Q.-P. Ding, N. Higa, N. S. Sangeetha, D. C. Johnston, and Y. Furukawa

Phys. Rev. B **95**, 184404 — Published 5 May 2017

DOI: 10.1103/PhysRevB.95.184404

NMR Determination of an Incommensurate Helical Antiferromagnetic Structure in $EuCo_2As_2$

Q.-P. Ding,[1] N. Higa,[1,2] N. S. Sangeetha,[1] D. C. Johnston,[1] and Y. Furukawa[1]

[1]*Ames Laboratory, U.S. DOE, and Department of Physics and Astronomy, Iowa State University, Ames, Iowa 50011, USA*
[2]*Department of Physics and Earth Sciences, Faculty of Science, University of the Ryukyus, Okinawa 903-0213, Japan*

(Dated: April 13, 2017)

We report ^{153}Eu, ^{75}As and ^{59}Co nuclear magnetic resonance (NMR) results on $EuCo_2As_2$ single crystal. Observations of ^{153}Eu and ^{75}As NMR spectra in zero magnetic field at 4.3 K below an antiferromagnetic (AFM) ordering temperature $T_N = 45$ K and its external magnetic field dependence clearly evidence an incommensurate helical AFM structure in $EuCo_2As_2$. Furthermore, based on ^{59}Co NMR data in both the paramagnetic and the incommensurate AFM states, we have determined the model-independent value of the AFM propagation vector $\mathbf{k} = (0, 0, 0.73 \pm 0.07)2\pi/c$ where c is the c lattice parameter. Thus the incommensurate helical AFM state was characterized by only NMR data with model-independent analyses, showing NMR to be a unique tool for determination of the spin structure in incommensurate helical AFMs.

PACS numbers: 75.25.-j, 75.50.Ee, 76.60.-k

I. INTRODUCTION

Understanding the magnetism in AFe_2As_2 (A = Ca, Ba, Sr, Eu) known as "122" compounds with a $ThCr_2Si_2$-type structure at room temperature became one of the important issues after the discovery of iron-pnictide superconductors [1–4]. These systems undergo coupled structural and magnetic phase transitions at a system-dependent Néel temperature T_N, below which long-range stripe-type antiferromagnetic (AFM) order emerges originating from Fe 3d electron spins. Superconductivity (SC) in these compounds emerges upon suppression of the stripe-type AFM phase by application of pressure and/or carrier doping. Because of the proximity between the AFM and the SC phases, it is believed that stripe-type AFM spin fluctuations play an important role in driving the SC in the iron-based superconductors, although orbital fluctuations are also pointed out to be important [5]. Recently ferromagnetic (FM) correlations were revealed to also play an important role in the iron-based superconductors [2, 6–9].

$EuFe_2As_2$, which exhibits SC under the application of 2–3 GPa of pressure and/or carrier doping [10, 11], is a special member in the "122" class of compounds, as Eu^{2+} has a large magnetic moment ($J = S = 7/2$, $L = 0$), where J, S, and L are the total, spin and orbital angular momenta, respectively. $EuFe_2As_2$ exhibits the stripe-type AFM order at 186 K due to the Fe spins, while the Eu^{2+} moments order antiferromagnetically below 19 K with an A-type AFM structure where the Eu ordered moments are FM aligned in the ab plane but the moments in adjacent layers along the c axis are antiferrmagnetically aligned [12]. With substitution of Co atoms for the Fe atoms in $Eu(Fe_{1-x}Co_x)_2As_2$, the ground-state magnetic structure of the Eu^{2+} spins is found to develop from the A-type AFM order in the parent compound, via the A-type canted AFM structure with some net FM moment component along the crystallographic c direction at intermediate Co doping levels around $x \sim 0.1$, and then to the pure FM order along the c axis at $x \sim 0.18$ (Ref. 11). With further substitution up to $x = 1$, $EuCo_2As_2$ is reported to again exhibit A-type AFM order of the Eu ordered moments below $T_N \sim 40$ K [13, 14], similar to the parent compound. On the other hand, recent neutron diffraction (ND) measurement reported a planar helical AFM structure below 47 K where the Eu ordered moments are aligned in the ab plane with the helical axis along the c axis [15]. Therefore, it is important to elucidate the magnetic state of Eu in $EuCo_2As_2$ by using different experimental techniques.

Nuclear magnetic resonance (NMR) is a powerful technique to investigate magnetic properties of materials from a microscopic point of view. In particular, one can obtain direct and local information of magnetic state at nuclear sites. Although Eu, Co and As are NMR active nuclei in $EuCo_2As_2$, there have been no NMR studies of this compound up to now to our knowledge.

In this paper, we have carried out NMR measurements to investigate the magnetic and electronic states of each ion in $EuCo_2As_2$, where we succeeded in observing NMR signals from all three ^{151}Eu, ^{59}Co and ^{75}As nuclei. From the external field dependence of ^{153}Eu and ^{75}As NMR spectra at 4.3 K, below $T_N = 45$ K an incommensurate helical AFM state shown in Fig. 1(a) was clearly evidenced in $EuCo_2As_2$. Furthermore, the AFM propagation vector characterizing the helical AFM state is determined to be $\mathbf{k} = (0, 0, 0.73 \pm 0.07)2\pi/c$ from the internal magnetic induction at the Co site obtained by ^{59}Co NMR under zero magnetic field. ^{59}Co NMR revealed that no magnetic ordering of the Co 3d electron spins occurs in the helical AFM state, evidencing that the magnetism in $EuCo_2As_2$ originates from only the Eu spins. These

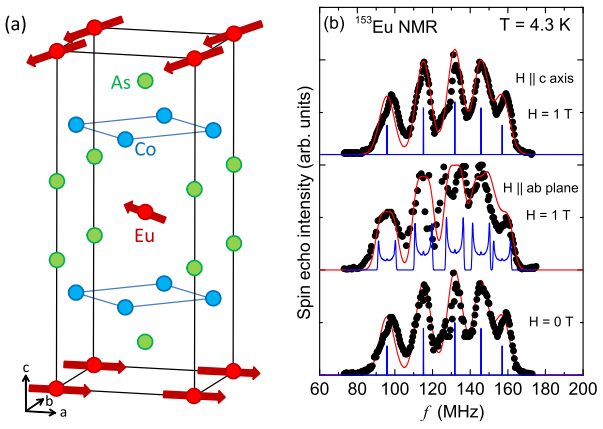

FIG. 1: (Color online) (a) Crystal and magnetic structures of $EuCo_2As_2$. (b) ^{153}Eu-NMR spectra at $T = 4.3$ K in the AFM state for $EuCo_2As_2$ in $H = 0$ (bottom), $H = 1$ T parallel to the ab plane (middle) and parallel to the c axis (top). The red and blue lines are the calculated ^{153}Eu NMR spectra with and without a distribution of $B_{\rm int}^{\rm Eu}$, respectively.

results are consistent with the recent neutron diffraction measurements [15].

II. EXPERIMENT

A single crystal ($9 \times 8 \times 1$ mm^3) of $EuCo_2As_2$ for the NMR measurements was grown using Sn flux [16]. NMR measurements of ^{153}Eu ($I = \frac{5}{2}$, $\frac{\gamma_N}{2\pi} = 4.632$ MHz/T, $Q = 2.49$ barns), ^{59}Co ($I = \frac{7}{2}$, $\frac{\gamma_N}{2\pi} = 10.03$ MHz/T, $Q = 0.4$ barns), and ^{75}As ($I = \frac{3}{2}$, $\frac{\gamma_N}{2\pi} = 7.2919$ MHz/T, $Q = 0.29$ barns) nuclei were conducted using a home-made phase-coherent spin-echo pulse spectrometer. In the AFM state, ^{153}Eu, ^{75}As and ^{59}Co NMR spectra in zero and nonzero magnetic fields H were measured in steps of frequency f by measuring the intensity of the Hahn spin echo. In the paramagnetic (PM) state, ^{59}Co NMR spectra were obtained by sweeping the magnetic field at $f = 51.1$ MHz. The ^{75}As nuclear spin-lattice relaxation rate $1/T_1$ was measured with a saturation recovery method [17].

III. RESULTS AND DISCUSSION

At the bottom panel of Fig. 1(b) the ^{153}Eu NMR spectrum in the AFM state for $EuCo_2As_2$ is shown, measured in zero magnetic field at a temperature $T = 4.3$ K. The observed spectrum is well reproduced by the following nuclear spin Hamiltonian which produces a spectrum with a central transition line flanked by two satellite peaks on both sides for $I = 5/2$, $\mathcal{H} = -\gamma\hbar\mathbf{I}\cdot\mathbf{B}_{\rm int} + \frac{h\nu_Q}{6}[3I_z^2 - I(I+1) + \frac{1}{2}\eta(I_+^2 + I_-^2)]$, where $B_{\rm int}$ is the internal magnetic induction at the Eu site, h is Planck's constant, and ν_Q is nuclear quadrupole frequency defined by $\nu_Q = 3e^2QV_{ZZ}/2I(2I-1)h$ ($= 3e^2QV_{ZZ}/20h$ for $I = 5/2$) where Q is the electric quadrupole moment of the Eu nucleus, V_{ZZ} is the electric field gradient (EFG) at the Eu site, and η is the asymmetry parameter of the EFG [18]. Since the Eu site in $EuCo_2As_2$ has a tetragonal local symmetry ($4/mmm$), η is zero. The blue lines shown at the bottom panel of Fig. 1(b) are the calculated positions for ^{153}Eu zero-field NMR (ZFNMR) lines using the parameters $|B_{\rm int}^{\rm Eu}| = 27.5(1)$ T, $\nu_Q = 30.6(1)$ MHz and $\theta = 90°$. Here θ represents the angle between $B_{\rm int}^{\rm Eu}$ and the principle axis of the EFG tensor at the Eu sites. As shown by the red curve in the figure, the observed ^{153}Eu ZFNMR spectrum was well reproduced with a broadening of ~ 1.1 T of the calculated lines originated from a distribution of $B_{\rm int}$ probably due to Eu ordered moment distributions.

Since $B_{\rm int}^{\rm Eu}$ is perpendicular to the c axis as will be shown below, the principle axis of the EFG is found to be the c axis, which is similar to the case of the Eu nucleus in $EuGa_4$ with the same $ThCr_2Si_2$-type crystal structure in which the similar values of $B_{\rm int}^{\rm Eu} = 27.08$ T and $\nu_Q = 30.5$ MHz for ^{153}Eu have been reported [19]. $B_{\rm int}^{\rm Eu}$ is proportional to $A_{\rm hf}<\mu>$ where $A_{\rm hf}$ is the hyperfine coupling constant and $<\mu>$ is the ordered Eu magnetic moment. The hyperfine field at the Eu sites mainly originates from core polarization from $4f$ electrons and is oriented in a direction opposite to that of the Eu moment [20]. For $|B_{\rm int}^{\rm Eu}| = 27.5(1)$ T and the reported AFM ordered moment $<\mu> = 7.26(8)$ μ_B/Eu from ND [15], $A_{\rm hf}$ is estimated to be -3.78 T/μ_B where the sign is reasonably assumed to be negative due to the core-polarization mechanism. The estimated $A_{\rm hf}$ is not far from the core-polarization hyperfine coupling constant -4.5 T/μ_B estimated for Eu^{2+} ions [20]. The small difference could be explained by a positive hyperfine coupling contribution due to conduction electrons which cancel part of the negative core polarization field.

In order to determine the direction of $B_{\rm int}^{\rm Eu}$ with respect to the crystal axes, we measured ^{153}Eu NMR in the single crystal in nonzero H. When H is applied along the c axis, almost no change of the ^{153}Eu NMR spectrum is observed [see the top panel in Fig. 1(b) where the simulated spectra shown by blue and red lines are the same as the case of $H = 0$]. This indicates that H is perpendicular to the ordered Eu moments and thus to $B_{\rm int}^{\rm Eu}$. Since the effective field at the Eu site is given by the vector sum of $\mathbf{B}_{\rm int}^{\rm Eu}$ and $\mathbf{H}$, i.e., $|\mathbf{B}_{\rm eff}| = |\mathbf{B}_{\rm int}^{\rm Eu} + \mathbf{H}|$, the resonance frequency is expressed for $H \perp <\mu>$ as $f = \frac{\gamma_N}{2\pi}\sqrt{(B_{\rm int}^{\rm Eu})^2 + H^2}$. For our applied field range where $B_{\rm int}^{\rm Eu} >> H$, any shift in the resonance frequency due to H would be small, as observed.

In the case of $\mathbf{H}$ applied perpendicular to the c axis, on the other hand, each line broadens as shown in the middle panel of Fig. 1(b). The broadening of each line cannot be explained by the A-type AFM state. In this

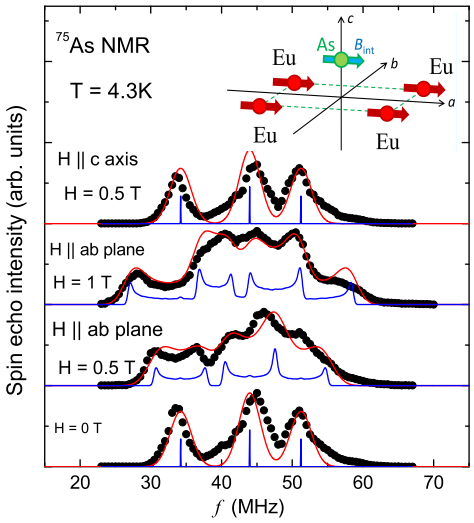

FIG. 2: (Color online) ^{75}As-NMR spectra at $T = 4.3$ K in the AFM state for $EuCo_2As_2$ in zero magnetic field, and magnetic fields parallel to the ab plane and parallel to the c axis. The red and blue lines are the calculated ^{75}As-NMR spectra with and without a distribution of $B_{\rm int}^{\rm As}$, respectively. The inset shows the coordination of nearest-neighbor Eu sites around an As site. The arrows on the Eu and As atoms indicate the directions of the Eu ordered moments and the internal magnetic induction at the As site, respectively.

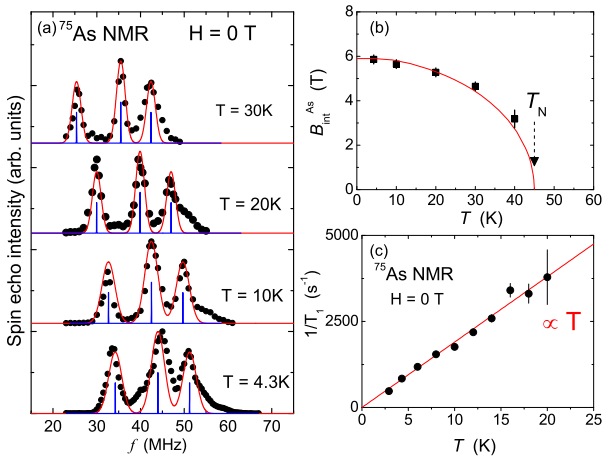

FIG. 3: (Color online) (a) Temperature dependence of ^{75}As-NMR spectra in zero magnetic field in the AFM state. The red and blue lines are the calculated ^{75}As-NMR spectra. (b) Temperature dependence of $B_{\rm int}^{\rm As}$. The solid curve is the Brillouin function with $J = S = 7/2$. (c) Temperature dependence of ^{75}As-NMR $1/T_1$ under zero magnetic field. The straight line shows the Korringa relation $1/T_1 = 190\ T$ (s^{-1}).

case, one expects a splitting of each line into two lines corresponding to two Eu planes where the Eu ordered moments are parallel or antiparallel to **H**. In order to explain the observed spectrum, we consider a planar helical structure which produces a two dimensional powder pattern. The blue solid line is a calculated spectrum for an incommensurate helical AFM state. With the inhomogeneous magnetic broadening due to the same distribution of $B_{\rm int}^{\rm Eu}$ as in the $H = 0$ T spectrum, the observed spectrum at $H = 1$ T is reasonably reproduced as shown by the red solid curve. Thus these NMR results reveal an incommensurate helical spin structure with the ordered moments aligned in the ab plane, consistent with recent ND measurements [15]. The observed ab-plane alignment of the ordered moments is also consistent with the prediction of the moment alignment from magnetic dipole interactions between the Eu spins [21]. A similar incommensurate helical spin structure has been reported in $EuCo_2P_2$ [22, 23].

The incommensurate planar helical structure is also revealed by ^{75}As NMR measurements. The bottom panel in Fig. 2 shows the ^{75}As ZFNMR spectrum at 4.3 K in the AFM state, where the blue lines are the expected positions for the three lines (for $I = 3/2$) calculated with the parameter $|B_{\rm int}^{\rm As}| = 5.86$ T, $\nu_{\rm Q} = 17.0$ MHz and $\theta = 90°$. As in the case of the ^{153}Eu ZFNMR spectrum, the observed ^{75}As ZFNMR spectrum is well reproduced with an inhomogeneous magnetic broadening of 4 kOe, as shown by the red curve. The distribution of $B_{\rm int}^{\rm As}$ originates from the distributions of the Eu ordered moments and its directions. When **H** is applied along the c axis, almost no change of the spectrum is observed as typically shown in the top panel of Fig. 2 where $H = 0.5$ T. This indicates that **H** is perpendicular to $\mathbf{B}_{\rm int}$ at the As site. On the other hand, when **H** is applied parallel to the ab plane, similar to the case of ^{153}Eu ZFNMR spectrum, each line broadens and exhibits a characteristic shape, again expected for the incommensurate planer helical AFM state.

According to Yogi *et al.*, the direction of $B_{\rm int}^{\rm As}$ is parallel to the Eu ordered moments in the case where the Eu ordered moments are ferromagnetically aligned in the Eu plane [19]. Therefore, one can expect almost no change of the ^{75}As ZFNMR spectrum when H is perpendicular to the Eu ordered moment, as observed in the ^{75}As ZFNMR spectrum for $H \parallel c$ axis. On the other hand, if one applies $H \parallel ab$ plane, a splitting of the ^{75}As ZFNMR spectrum is expected similar to the case of the ^{153}Eu ZFNMR spectrum. The blue lines in the two middle panels of Fig. 2 are calculated spectra of ^{75}As NMR for the planar helical AFM structure under $H = 0.5$ T and 1 T. With the same inhomogeneous magnetic broadening (~ 4 kOe) due to a distribution of $B_{\rm int}^{\rm As}$, both spectra are well reproduced as shown by the red curves.

The T dependence of the ^{75}As ZFNMR spectrum is shown in Fig. 3(a). With increasing T, the spectra shift to lower frequency due to reduction of the internal magnetic induction $|B_{\rm int}^{\rm As}|$ which decreases from 5.86 T at 4.3 K to 3 T at 40 K. No obvious change in $\nu_{\rm Q} = 17.0$ MHz is observed. The T dependence of $|B_{\rm int}^{\rm As}|$ shown in Fig. 3(b), which is the T dependence of the order pa-

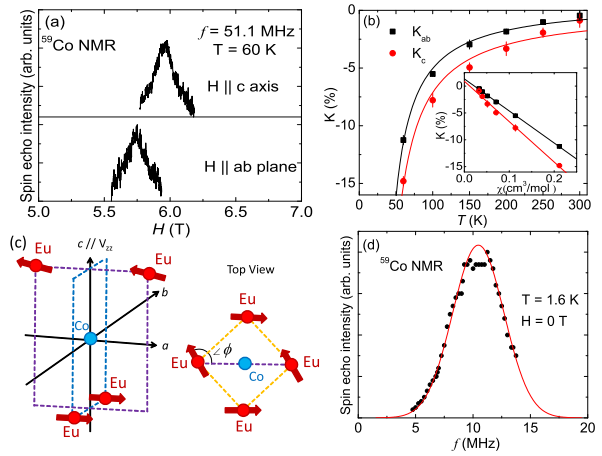

FIG. 4: (Color online) (a) Field-swept ^{59}Co-NMR spectra of $EuCo_2As_2$ for $H \parallel ab$ plane (bottom) and $H \parallel c$ axis (top) measured at f = 51.1 MHz and T = 60 K. (b) Temperature dependence of ^{59}Co Knight shifts K_{ab} and K_c in the paramagnetic state. The solid curves are fits to the data by Curie-Weiss law. The inset shows $K(T)$ versus magnetic susceptibility $\chi(T)$ for the corresponding ab and c components of K. The solid lines are linear fits. (c) Coordination of nearest-neighbor Eu sites around Co site. The arrows on the Eu atoms indicate the ordered magnetic moments. The magnetic moment turn angle between adjacent magnetic layers is ϕ. (d) ^{59}Co-NMR spectrum at T = 1.6 K in the AFM state in zero magnetic field.

rameter of the planar helical AFM state, is well reproduced by a Brillouin function which was calculated based on the Weiss molecular field model with $J = S = 7/2$, T_N = 45 K and H_{int}^{As} = 5.86 T. This indicates that the magnetic state of the Eu ions is well explained by the local moment picture although the system is metallic as determined from electrical resistivity measurements [16]. The metallic ground state was confirmed by the T dependence of $1/T_1$ measured at the central line of the ^{75}As-ZFNMR spectrum. As shown in Fig. 3(c), $1/T_1$ is proportional to T, thus obeying a Korringa law $1/T_1T$ = 190 (sK)$^{-1}$. This confirms a metallic state from a microscopic point of view.

Now we discuss our ^{59}Co NMR data for both the PM and AFM ordered states. Figure 4(a) shows the field-swept ^{59}Co NMR spectra in the PM state at T = 60 K for $H \parallel c$ and $H \parallel ab$. For $I = 7/2$ nuclei, one expects a central transition line with three satellite lines on both sides. The observed spectra, however, do not show the seven distinct lines but rather exhibit a single broad line due to inhomogeneous magnetic broadening. The T dependence of the NMR shift for $H \parallel c$ (K_c) and $H \parallel ab$ (K_{ab}) is shown in Fig. 4(b), where we fit the data with the Curie-Weiss law $\frac{C}{T-\theta_p}$. The solid curves are fits with C = −553 (−440) %K and θ_p = 24.0 (24.0) K for K_c (K_{ab}). The values θ_p = 24.0 K for both field directions indicate predominant FM exchange interactions between Eu spins. This is consistent with the in-plane FM exchange interactions responsible for the planar helical AFM structure.

The hyperfine coupling constants A_{ab} and A_c for ^{59}Co surrounded by four Eu^{2+} ions can be estimated from the slopes of K-χ plots with the relation $A = \frac{N_A}{Z}\frac{K(T)}{\chi(T)}$, where N_A is Avogadro's number and $Z = 4$ is the number of nearest-neighbor Eu^{2+} ions around a Co atom. As shown in the inset of Fig. 4(b), both K_{ab} and K_c vary linearly with the corresponding χ. From the respective slopes, we estimate A_{ab} = (−0.875 ± 0.09) kOe/μ_B/Eu and A_c = (−1.09 ± 0.17) kOe/μ_B/Eu, respectively. These values are much smaller than a typical value A = −105 kOe/μ_B for Co 3d electron core polarization [20]. This indicates that the hyperfine field at the Co site originates from the transferred hyperfine field produced by the Eu^{2+} spins and that no 3d spins on the Co sites contribute to the magnetism of $EuCo_2As_2$.

We now consider the influence of the planar helical AFM state on the Co NMR data. We have succeeded in observing the ^{59}Co ZFNMR spectrum at 4.3 K as shown in Fig. 4(d), where the internal magnetic induction at the Co site is estimated to be $|B_{int}^{Co}|$ = 10.3 kOe. Based on the analysis for B_{int} by Yogi *et al.* for $EuGa_4$ (Ref. 19), we extended their calculation of B_{int} to an incommensurate helical AFM state and found that $|B_{int}|$ at the Co site appears in only the ab plane when the Eu ordered moments lie in the ab plane and is expressed by

$$B_{int}^{Co} = 2\langle\mu\rangle A_{ab}\sqrt{2+2\cos\phi} \qquad (1)$$

where ϕ is the turn angle along the the c axis between the Eu ordered moments in adjacent Eu planes, which characterizes the helical structure. In the case of $\phi = \pi$ corresponding to an A-type collinear AFM state, B_{int}^{Co} is zero due to a cancellation of the internal magnetic induction from the four nearest-neighbor Eu ordered moments. On the other hand, if ϕ deviates from π corresponding to a helical state, one can expect a finite B_{int}^{Co}. Thus the observation of the finite B_{int}^{Co} is direct evidence of the planar incommensurate helical AFM state in $EuCo_2As_2$. Furthermore, using Eq. (1), we can determine the AFM propagation vector $\mathbf{k}$ = (0, 0, k)2π/c, where c is the c-axis lattice parameter of the body-centered tetragonal Eu sublattice. Since the distance d along the c axis between adjacent layers of FM-aligned Eu moments is $d = c/2$, the turn angle between the ordered moments in adjacent Eu layers is $\phi = kd$, as shown in Fig. 4(c). Using $\langle\mu\rangle$ = 7.26(8) μ_B [15], A_{ab} = −0.875 kOe/μ_B/Eu and B_{int}^{Co} = 10.3 kOe, the turn angle ϕ is estimated to be 132° corresponding to a helical wave vector $\mathbf{k}$ = (0, 0, 0.73 ± 0.07)2π/c. This value of $\mathbf{k}$ is in very good agreement with $\mathbf{k}$ = (0, 0, 0.79)2π/c obtained from ND data [15].

IV. SUMMARY

In summary, we have shown that by analyzing the NMR spectrum in zero field and its external-field dependence, one can determine directly an incommensurate helical AFM structure in $EuCo_2As_2$. The AFM propagation vector characterizing the incommensurate helical AFM state was determined model-independently to be $\mathbf{k} = (0, 0, 0.73 \pm 0.07)2\pi/c$ from the internal magnetic field at the Co site obtained by ^{59}Co NMR under zero magnetic field. Thus NMR can be a unique tool for a model-independent determination of the spin structure in incommensurate helical antiferromagnets. This should prove valuable for the future investigation of local spin configurations in other europium compounds such as in $EuCo_2P_2$ which is also reported to exhibit an incommensurate helical AFM structure below 66 K [22, 23]. Our NMR approach can also be used to study in detail the magnetism originating from the Eu spins in $Eu(Fe_{1-x}Co_x)_2As_2$ SCs where the magnetic structure of the Eu spins changes from the A-type AFM state to a canted AFM state, and then to the ferromagnetic state with increasing Co substitution [11]. Such a detailed study would provide clues about the origin of the coexistence of SC and magnetism in the $Eu(Fe_{1-x}Co_x)_2As_2$ system.

V. ACKNOWLEDGMENTS

The authors thank Mamoru Yogi at University of the Ryukyus for helpful discussions. The research was supported by the U.S. Department of Energy, Office of Basic Energy Sciences, Division of Materials Sciences and Engineering. Ames Laboratory is operated for the U.S. Department of Energy by Iowa State University under Contract No. DE-AC02-07CH11358. N. H. thanks the Japan Society for the Promotion of Science KAKENHI : J-physics (Grant Nos. JP5K21732, JP15H05885, and JP16H01078) for financial support to be a visiting scholar at the Ames Laboratory.

[1] Y. Kamihara, T. Watanabe, M. Hirano, and H. Hosono, Iron-Based Layered Superconductor $La[O_{1-x}F_x]FeAs$ (x = 0.05-0.12) with T_c = 26 K, J. Am. Chem. Soc. **130**, 3296 (2008).

[2] D. C. Johnston, The puzzle of high temperature superconductivity in layered iron pnictides and chalcogenides, Adv. Phys. **59**, 803 (2010).

[3] P. C. Canfield and S. L. Bud'ko, FeAs-Based Superconductivity: A Case Study of the Effects of Transition Metal Doping on $BaFe_2As_2$, Annu. Rev. Condens. Matter Phys. **1**, 27 (2010).

[4] G. R. Stewart, Superconductivity in iron compounds, Rev. Mod. Phys. **83**, 1589 (2011).

[5] Y. K. Kim, W. S. Jung, G. R. Han, K.-Y. Choi, C.-C. Chen, T. P. Devereaux, A. Chainani, J. Miyawaki, Y. Takata, Y. Tanaka, M. Oura, S. Shin, A. P. Singh, H. G. Lee, J.-Y. Kim, and C. Kim, Existence of Orbital Order and its Fluctuation in Superconducting $Ba(Fe_{1-x}Co_x)_2As_2$ Single Crystals Revealed by X-ray Absorption Spectroscopy, Phys. Rev. Lett. **111**, 217001 (2013).

[6] Y. Nakai, K. Ishida, Y. Kamihara, M. Hirano, and H. Hosono, Spin Dynamics in Iron-Based Layered Superconductor $(La_{0.87}Ca_{0.13})FePO$ revealed by ^{31}P and ^{139}La NMR Studies, Phys. Rev. Lett. **101**, 077006 (2008).

[7] P. Wiecki, V. Ogloblichev, A. Pandey, D. C. Johnston, and Y. Furukawa, Coexistence of antiferromagnetic and ferromagnetic spin correlations in $SrCo_2As_2$ revealed by ^{59}Co and ^{75}As NMR, Phys. Rev. B **91**, 220406(R) (2015).

[8] P. Wiecki, B. Roy, D. C. Johnston, S. L. Bud'ko, P. C. Canfield, and Y. Furukawa, Competing Magnetic Fluctuations in Iron Pnictide Superconductors: Role of Ferromagnetic Spin Correlations Revealed by NMR, Phys. Rev. Lett. **115**, 137001 (2015).

[9] J. Cui, P. Wiecki, S. Ran, S. L. Bud'ko, P. C. Canfield, and Y. Furukawa, Coexistence of antiferromagnetic and ferromagnetic spin correlations in $Ca(Fe_{1-x}Co_x)_2As_2$ revealed by ^{75}As nuclear magnetic resonance, Phys. Rev. B **94**, 174512 (2016).

[10] T. Terashima, M. Kimata, H. Satsukawa, A. Harada, K. Hazama, S. Uji, H. S. Suzuki, T. Matsumoto, and K. Murata, $EuFe_2As_2$ under High Pressure: An Antiferromagnetic Bulk Superconductor, J. Phys. Soc. Jpn. **78**, 083701 (2009).

[11] W. T. Jin, Y. Xiao, Z. Bukowski, Y. Su, S. Nandi, A. P. Sazonov, M. Meven, O. Zaharko, S. Demirdis, K. Nemkovski, K. Schmalzl, L. M. Tran, Z. Guguchia, E. Feng, Z. Fu, and Th. Brückel, Phase diagram of Eu magnetic ordering in Sn-flux-grown $Eu(Fe_{1-x}Co_x)_2As_2$ single crystals, Phys. Rev. B **94**, 184513 (2016).

[12] H. S. Jeevan, Z. Hossain, D. Kasinathan, H. Rosner, C. Geibel, and P. Gegenwart, Electrical resistivity and specific heat of single-crystalline $EuFe_2As_2$: A magnetic homologue of $SrFe_2As_2$, Phys. Rev. B **78**, 052502 (2008).

[13] H. Raffius, E. Mörsen, B. D. Mosel, W. Müller-Warmuth, W. Jeitschko, L.Terbüchte, and T. Vomhof, Magnetic properties of ternary lanthanoid transition metal arsenides studied by Mössbauer and susceptibility measurements, J. Phys. Chem. Solids **54**, 135 (1993).

[14] J. Ballinger, L. E Wenger, Y. K. Vohra, and A. S. Sefat, Magnetic properties of single crystal $EuCo_2As_2$, J. Appl. Phys. **111**, 07E106 (2012).

[15] X. Tan, G. Fabbris, D. Haskel, A. A. Yaroslavtsev, H. Cao, C. M. Thompson, K. Kovnir, A. P. Menushenkov, R. V. Chernikov, V. O. Garlea, and M. Shatruk, A transition from localized to strongly correlated electron behavior and mixed valence driven by physical or chemical pressure in ACo_2As_2 (A = Eu and Ca), J. Am. Chem. Soc. **138**, 2724 (2016).

[16] N. S. Sangeetha and D. C. Johnston (unpublished).

[17] Nuclear spin-lattice relaxation rate $1/T_1$ at each T was determined by fitting the nuclear magnetization M versus time t using the exponential function $1 - M(t)/M(\infty) = 0.1e^{-t/T_1} + 0.9e^{-6t/T_1}$ for ^{75}As NMR, where $M(t)$ and $M(\infty)$ are the nuclear magnetization at

time t after saturation and the equilibrium nuclear magnetization at $t \to \infty$, respectively.

[18] C. P. Slichter, *Principles of Magnetic Resonance*, 3rd ed. (Springer, New York, 1990).

[19] M. Yogi, S. Nakamura, N. Higa, H. Niki, Y. Hirose, Y. Ōnuki, and H. Harima, ^{153}Eu and ^{69,71}Ga Zero-Field NMR Study of Antiferromagnetic State in $EuGa_4$, J. Phys. Soc. Jpn. **82**, 103701 (2013).

[20] A. J. Freeman and R. E. Watson, in *Magnetism*, edited by G. T. Rado and H. Suhl (Academic Press, New York, 1965), Vol. IIA, Ch. 4, pp. 167–305.

[21] D. C. Johnston, Magnetic dipole interactions in crystals, Phys. Rev. B **93**, 014421 (2016).

[22] M. Reehuis, W. Jeitschko, M. H. Möller, and P. J. Brown, A neutron diffraction study of the magnetic structure of $EuCo_2P_2$, J. Phys. Chem. Solids **53**, 687 (1992).

[23] N. S. Sangeetha, E. Cuervo-Reyes, A. Pandey, and D. C. Johnston, $EuCo_2P_2$: A model molecular-field helical Heisenberg antiferromagnet, Phys. Rev. B **94**, 014422 (2016).